Renewable Resource-Based Green Composites from Recycled Cellulose Fiber and Poly(3-hydroxybutyrate-*co*-3-hydroxyvalerate) Bioplastic

Rahul Bhardwaj,[†] Amar K. Mohanty,*[,†] L. T. Drzal,[‡] F. Pourboghrat,[§] and M. Misra[‡]

School of Packaging, 130 Packaging Building, Composite Materials and Structures Center, 2100 Engineering Building, and Department of Mechanical Engineering, 2555 Engineering Building, Michigan State University, East Lansing, Michigan 48824

Received November 24, 2005; Revised Manuscript Received February 23, 2006

Novel "green" composites were successfully fabricated from recycled cellulose fibers (RCF) and a bacterial polyester, poly(3-hydroxybutyrate-*co*-3-hydroxyvalerate) (PHBV) by melt mixing technique. Various weight contents (15%, 30%, and 40%) of the fibers were incorporated in the PHBV matrix. The effect of the fiber weight contents on the thermal, mechanical, and dynamic−mechanical thermal properties of PHBV was investigated and a comparative property analysis was performed with RCF-reinforced polypropylene (PP) composites. The tensile and storage moduli of the PHBV-based composites were improved by 220% and 190%, respectively, by reinforcement with 40 wt % RCF. Halpin−Tsai and Tsai−Pagano's equations were applied for the theoretical modeling of the tensile modulus of PHBV-based composites. The heat deflection temperature (HDT) of the PHBV-based composites was increased from 105 to 131 °C, while the coefficient of linear thermal expansion (CLTE) value was reduced by 70% upon reinforcement with 40 wt % RCF. The PHBV-based composites had also shown better tensile and storage moduli and lower CLTE values than PP-based composites. Differential scanning calorimetry (DSC), thermogravimetric analysis (TGA), and scanning electron microscopy (SEM) were used to study the melting behavior, thermal stability, and morphology of the composite systems, respectively.

Introduction

Natural fiber-reinforced thermoplastics are envisioned as an emerging new class of benign composite materials. The prospective benefits of these composites are derived from the properties of the natural fibers such as renewability, biodegradability, low cost, low density, acceptable specific mechanical properties, ease of separation, and carbon dioxide sequestration.[1] Natural fibers are looked upon as an ecofriendly and economical alternate to glass fibers. Natural fiber-reinforced composites are making inroads in many applications areas such as automobile, housing, and packaging. Natural fiber-reinforced composites having conventional polyolefins as matrices, that is, polypropylene (PP) and polyethylene (PE) have been extensively researched.[2−4] The nonbiodegradability of conventional polymers and exhausting petroleum resources has triggered the extensive research and development in the field of biobased polymers and their applications. There is a great interest in developing ecofriendly green composites/biocomposites from plant-derived bio/natural fibers and crop-derived bioplastics due to their renewable resource-based origin and biodegradable nature.[5−6]

Polyhydroxyalkanoates (PHAs), also known as bacterial polyester, have shown a lot of promise as novel materials due to their renewability, biodegradability, and biocompatibility.[7] Poly(3-hydroxybutyrate) (PHB) and poly(3-hydroxybutyrate-*co*-3-hydroxyvalerate) (PHBV) are the main representatives of the polyhydroxyalkanoates (PHAs). PHB is a highly crystalline and brittle polymer but possesses melting point and mechanical properties comparable to those of isotactic polypropylene (iPP).[8−9] PHB-based copolymers are being developed to overcome the shortcomings of PHB. PHBV is a copolymer (Chart 1) consisting of randomly arranged (*R*)-3-hydroxybutyrate (HB) and (*R*)-3-hydroxyvalerate (HV) units.[10] PHBV has a lower melting point and higher flexibility than the homopolymer, poly(3-hydroxybutyrate) (PHB).[10] The lower melting point of PHBV improves the melt stability and broadens the processing window of this polymer.[11] The amount of hydroxyvalerate (HV) content in the PHBV copolymer strongly influences the properties of this polymer such as crystallinity, melting point, and crystallization rate.[12] The major drawbacks of PHBV are the development of interlamellar secondary crystallization on storage, slow crystallization rate, and high production cost.[13−14] Bio/natural fibers have been incorporated in the PHBV matrix to improve its thermomechanical properties and cost reduction of the final product.[15−17] The use of recycled cellulose fibers such as wood flour and newspaper fibers as reinforcing filler has been reported for thermoplastics such as polypropylene (PP) and high-density polyethylene (HDPE).[18−19] The usage of recycled cellulose fibers in value-added applications can help in reducing municipal solid waste (MSW), sustaining the recycling industries and forest products, and reducing the cost of the molded product. Huda et al.[20,21] recently reported the improved thermomechanical properties of poly(lactic acid)- (PLA-) based green composite reinforced with recycled newspaper fibers. The recycled cellulose fiber- (RCF-) reinforced PHBV composite can be a novel

Chart 1. Chemical Structure of PHBV Copolymer

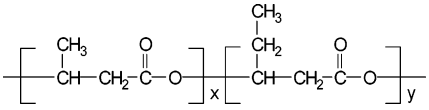

* To whom correspondence should be addressed: e-mail mohantya@msu.edu; telephone +1-517-355-3603; fax +1-517-353-8999.

[†] School of Packaging.

[‡] Composite Materials and Structures Center.

[§] Department of Mechanical Engineering.

10.1021/bm050897y CCC: $33.50 © 2006 American Chemical Society
Published on Web 04/26/2006

Table 1. Processing Parameters of PHBV, PP, and Their Composites

	processing temp (°C) at three sections of miniextruder			
material type	top	center	bottom	cycle time (min)
PHBV/RCF (100/0)	155	160	155	3
PHBV/RCF (85/15)	155	160	155	6
PHBV/RCF (70/30)	155	160	155	8
PHBV/RCF (60/40)	155	160	155	8
PP/RCF (100/0)	190	190	190	3
PP/RCF (70/30)	190	190	190	10
PP/RCF (60/40)	190	190	190	10

material due to the lower processing temperature of PHBV, which can avoid thermal degradation of the cellulosic fibers. The polar nature of the PHBV copolymer is also expected to provide better dispersion and interfacial adhesion with polar cellulosic fibers as compared to the nonpolar PP and HDPE.

This paper presents the fabrication of green composite from recycled cellulose fibers (mixture of newspaper, magazine, and kraft paper fibers) and poly(3-hydroxybutyrate-*co*-3-hydroxyvalerate) by the melt mixing technique. Effect of fiber weight contents on the mechanical, thermomechanical, and dynamical mechanical thermal properties of PHBV was studied. Recycled cellulose fiber-reinforced polypropylene (PP) composites were also fabricated by a similar technique, and a comparative property analysis for the two composite systems was performed.

Experimental Section

Materials. Poly(3-hydroxybutyrate-*co*-3-hydroxyvalerate), PHBV, trade name Biopol (Zeneca Bio Products), molecular weight − 450 000, 13% valerate content, was procured from Biomer, Germany. Basell Polyolefins, Elkton, MD, supplied Profax 6523, a polypropylene (PP) homopolymer. The melt flow index (MFI) of polypropylene was 4.0 g/10 min. CreaFill Fibers Corp., Chestertown, MD, supplied recycled cellulose fiber (RCF), trade name CreaMix TC 1004. It was a mixed fiber reclaimed from selected newspapers, magazines, or kraft paper stock.[22] The average fiber length and width were 800 and 20 μm, respectively. The constituents of recycled cellulose fiber were cellulose 75%, ash 23%, and others 2%. The ash was the carbon left after burning, and others included organics/ nonorganics such as clays, lignin, inks, tannins, extractives, etc. The moisture content of fibers was less than 5%.

Composite Fabrication. PHBV and RCF were dried for 3 and 18 h, respectively, at 80 °C in a vacuum oven before the processing. Polypropylene was not dried before processing. The composites were fabricated by extrusion followed by injection molding process. The processing was performed in a microcompounding instrument (DSM Research, Netherlands). The instrument is a corotating twin-screw microcompounder having screw length of 150 mm, L/D of 18, and barrel volume of 15 cm^3. The molten composite material was transferred from a miniextruder to a preheated small injection molder for fabrication of various test specimens. The PHBV-based composite formulations contained 15, 30, and 40 wt % RCF, while the PP-based composites contained 30 and 40 wt % RCF. The processing parameters for PHBV, PP, and their composite system are depicted in Table 1. The material type represents compositions in weight/weight. The processing temperature represents the temperature profile of a perpendicular barrel at top, center, and bottom sections. The processing temperature and residence time have significant effects on the mechanical properties of the PHBV. The processing temperature of PHBV and its composites was kept below 170 °C due to its degradation above this temperature.[23] The temperature of the barrel at the bottom section and of the injection molder (155 °C) was kept below the melting point of PHBV (157 °C) to improve the melt stability of the PHBV. PHBV also remains in the molten state for a sufficient period of time below its melting point due to its slow crystallization rate.[23] The processing cycle time for composite systems having higher recycled cellulose fiber weight content was increased to allow the efficient dispersion of fibers in the respective matrix.

Testing and Characterization: *Thermal Properties.* Differential scanning calorimetry (DSC) of the neat polymers and their composite systems was performed with DSC Q100, TA Instruments. The heat/cool/heat method was chosen for all samples. All samples were heated to 190 °C with a ramp of 10 °C/min to erase the thermal history. The data for glass transition temperature and melting points were collected during the second heating cycle having a ramp of 10 °C/min up to 190 °C. The crystallization temperature was obtained from the cooling cycle. Thermogravimetric analysis (TGA) was performed on a thermogravimetric analyzer (TGA 2950). The heating rate of 20 °C/min was chosen for all samples.

Thermomechanical Properties. The storage modulus of the neat polymers and their composites was evaluated with DMAQ800, TA Instruments. The test was carried out by heating the samples at a rate of 2 °C/min from 30 to 80 °C. The samples were tested in a single cantilever mode at an oscillating amplitude of 15 μm and frequency of 1 Hz. Heat deflection temperature (HDT) of the neat polymers and their composites was measured by using DMA Q800 as per ASTM D648. The rectangular bars of nominal size 1.99 mm × 12 mm × 58 mm were used for testing. The three-point bending mode was used to apply a load of 66 psi. The samples were heated at the rate of 2 °C/min from room temperature to the desired temperature. Coefficient of linear thermal expansion (CLTE) is the ratio of change in length per kelvin to the length at 273 K. It is obtained from $l = lt(1 + \alpha\Delta t)$; here α is the coefficient of linear thermal expansion, and l and lt and are the initial length of sample and its length after a temperature t, respectively. Δt is the change in temperature. Coefficient of linear thermal expansion (CLTE) of the neat polymers and their composites was determined by use of a TMA 2940 thermomechanical analyzer with an expansion probe. The samples were heated at the rate of 3 °C/min from 30 to 90 °C.

Mechanical Properties. Tensile properties were measured with the help of United Calibration Corp. SFM 20 testing machine as per ASTM D638. The specimens were tested at a crosshead speed of 50 mm/min. The notched izod impact strength was measured with Inc. (TMI) 43-02-01 monitor/impact machine according to ASTM D256. The impact energy of the pendulum was 1 ft-lb.

Morphological Studies. A JEOL scanning electron microscope (model JSM-6400) was used to evaluate the morphology of the impact-fractured surfaces of the composites. The samples were sputter-coated with gold particles up to a thickness of ~10 nm before the surface characterization. The SEM instrument has a lanthanum hexaboride (LaB_6) crystal as electron emitter. An accelerating voltage of 15 kV was used to collect the SEM photomicrographs.

Results and Discussion

Differential Scanning Calorimetry. The differential scanning calorimetry (DSC) of recycled cellulose fiber-reinforced PHBV composites was carried out to investigate their crystal-

Table 2. Detailed Information Obtained from Differential Scanning Calorimetry of PHBV and Its Composites[a]

type	fiber content (wt %)	T_g (°C)	melting points (°C) T_{m_1}	T_{m_2}	T_c (°C)	ΔH_f (J/g)	ΔH_c (J/g)
PHBV	0	0.3		157.3	112.8	61.9	55.3
PHBV/RCF	15	1.9		162.4	114.0	55.3	48.9
PHBV/RCF	30	2.6	143.5	155.6	88.0	33.7	34.1
PHBV/RCF	40	2.7	141.3	154.3	83.0	33.6	30.7

[a] Here T_g = glass transition temperature, T_{m_1} and T_{m_2} = melting points, T_c = crystallization temperature, ΔH_f = enthalpy of fusion, and ΔH_c = enthalpy of crystallization.

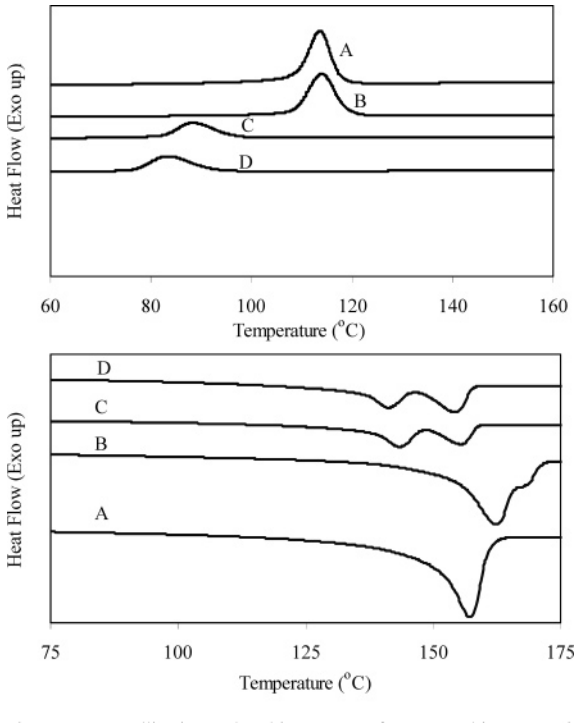

Figure 1. Crystallization and melting curves of PHBV and its composites: (A) PHBV/RCF (100/0); (B) PHBV/RCF (85/15); (C) PHBV/RCF (70/30); (D) PHBV/RCF (60/40).

lization and melting behavior. DSC curves of neat PHBV and composites are depicted in Figure 1, and the detailed information is shown in Table 2. The neat PHBV showed an endothermic peak corresponding to a melting point at 157 °C and an exothermic peak representing the crystallization temperature at 112.75 °C. Glass transition temperature (T_g) of PHBV was found to increase with addition of RCF in the PHBV matrix. The increase in T_g is possibly due to the hindrance caused by the rigid framework of RCF to the segmental mobility of polymer chains in PHBV. Shanks et al.[24] also reported a similar kind of observation pertaining to glass transition temperature of flax-biopolyester composite. The melting temperature (T_m) of the PHBV was increased from 157.3 to 162.4 °C with addition of 15 wt % RCF. Nucleation and crystal growth in PHBV is much slower than in PHB.[14] The fiber surface reduced the critical nucleus size required for the formation of a stable nucleus in PHBV, and this decrease in nucleus size had a more prominent effect in PHBV[15] at low fiber loading. The bimodal endothermic melting peaks were observed for PHBV with addition of 30 and 40 wt % RCF. The lower melting peaks, that is, T_{m_1} (Table 1), of the bimodal endotherms can be accounted to the melting of thin, unstable crystals formed due to the heterogeneous distribution of the crystals and nonuniform crystal thickness developed in PHBV due to the fiber hindrance, while T_{m_2} represents the true melting point of PHBV. Crystallization temperature of the PHBV and its composite was obtained from

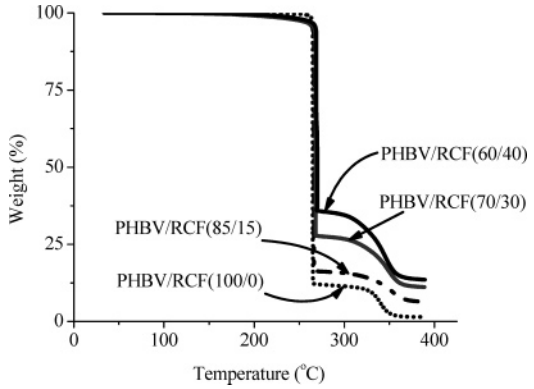

Figure 2. TGA curves of PHBV/RCF composites.

the cooling curve during differential scanning calorimetry (DSC). Crystallization temperature of the PHBV was slightly improved at 15 wt % RCF but reduced significantly at 30 and 40 wt % RCF. This is probably due to the confinement of the polymer chains caused by the large amount of fibers leading to the slower diffusion and migration of polymer chains to the surface of the nucleus, thus resulting in the decrease of crystallization temperature during cooling of PHBV-based composites containing 30 and 40 wt % RCF. There was a considerable decrease in the heat of fusion (ΔH_f) of the PHBV-based composites having 30 and 40 wt % RCF, respectively. The reduction in the free volume of PHBV caused by the large amount of RCF could have led to the limited growth of the PHBV spherulite, thus causing a depression in the heat of fusion (ΔH_f).

Thermogravimetric Analysis. Thermogravimetric analysis (TGA) of PHBV and its composites is shown in Figure 2. The TGA curves showed that PHBV-based composites undergo massive thermal degradation above 250 °C. The onset of thermal degradation of PHBV-based composites was similar to that of neat PHBV. This can be attributed to the fact that PHBV is thermally unstable and starts degrading drastically above 250 °C due to chain scission reactions leading to the reduction of molecular weight and resulting in the formation of the volatile acid products such as crotonic acid.[25] Crotonic acid is also supposedly known to cause hydrolysis of the cellulose content of natural fiber and result in defibrillation.[25] TGA curves of PHBV-based composite systems also suggested that there was no additional thermal degradation of PHBV with incorporation of RCF. There was formation of different amounts of residue in PHBV-based composites containing different amounts of RCF. The amount of residue was higher in composites having a higher amount of recycled cellulose fibers. One other reason for high residue in PHBV-based composite was due to the presence of high ash content (23%) in the RCF composition used in this study.

Figure 3 shows the comparative TGA curves of the PHBV- and PP-based composite systems having 40 wt % RCF content. The onset of thermal degradation in the PHBV-based composite

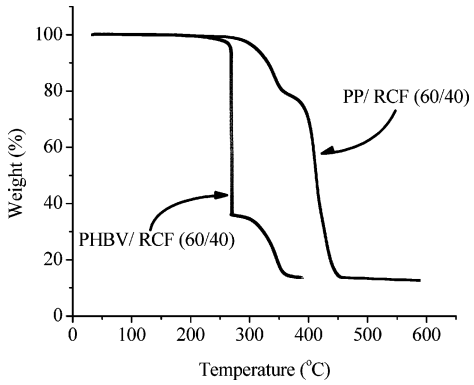

Figure 3. Comparative TGA curves of RCF-reinforced PHBV and PP composites.

Table 3: Comparative Storage Moduli of PHBV, PP, and Their Composites at Different Temperatures

	storage modulus *E* (MPa)		
type	30 °C	50 °C	70 °C
PHBV/RCF (100/0)	1186	882	540
PHBV/RCF (85/15)	1848	1414	943
PHBV/RCF (70/30)	2583	2039	1458
PHBV/RCF (60/40)	2990	2290	1705
PP/RCF (100/0)	1412	934	580
PP/RCF (70/30)	2403	1793	1258
PP/RCF (60/40)	2983	2287	1585

was comparable to that of the PP-based composite. But the degradation rate in RCF-reinforced PHBV composites was more drastic after 250 °C, which was due to the degradation of both recycled cellulose fiber and PHBV. In the case of RCF-reinforced PP composite, degradation was accelerated after 250 °C but the degradation rate was slow as compared to RCF-reinforced PHBV composites. The degradation in RCF-reinforced PP composite in this region was primarily due to degradation of the RCF.

Thermomechanical Properties: *Storage Modulus (E′).* Storage modulus represents the ratio of the in-phase stress to the applied strain, which is further related to the energy stored per cycle of deformation.[26] Storage modulus (*E′*) determines the dynamic rigidity of a material, which originates from the elastic response of the material. The temperature dependence of the storage moduli of PHBV, PP, and their composites is given in Table 3. The storage modulus values of the PHBV-based composite containing 30 and 40 wt % RCF was increased by 117% and 190%, respectively, as compared to neat PHBV at 30 °C. The PHBV-based composites had also shown higher storage moduli than PP-based composites at all fiber loadings even though the neat PHBV has a lower storage modulus, 1.1 GPa, as compared to neat PP, 1.4 GPa (Table 3). The higher *E′* values of PHBV-based composites as compared to PP-based composites could be due to the better compatibility and dispersion of RCF in PHBV-based composites as compared to PP-based composites. The relatively polar nature and presence of a carbonyl group (>C═O) in PHBV as compared to nonpolar PP might have caused hydrogen-bonding-type interaction with the cellulosic fibers. The *E′* values were decreased for all the composite systems with increasing temperature due to the softening of the PHBV and PP matrix. The PHBV-based composites showed fairly high *E′* values compared with the PP-based composites even at higher temperature (Table 3).

Heat Deflection Temperature. Figure 4 shows the values of heat deflection temperature (HDT) for PHBV, PP, and their

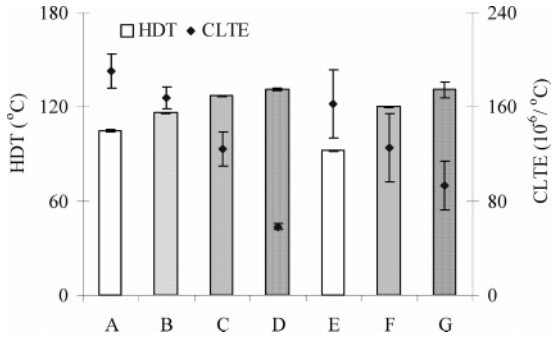

Figure 4. Heat deflection temperature (HDT) and coefficient of linear thermal expansion (CLTE) values of PHBV, PP, and their composites: (A) PHBV/RCF (100/0); (B) PHBV/RCF (85/15); (C) PHBV/RCF (70/30); (D) PHBV/RCF (60/40); (E) PP/RCF (100/0): (F) PP/RCF (70/30); (G) PP/RCF (60/40).

composites. HDT of both PHBV and PP was improved after the incorporation of RCF. The HDT value of virgin PHBV matrix was increased from 105 to 116, 127, and 131 °C with addition of 15, 30, and 40 wt % RCF. The HDT value of a material depends on the modulus and the glass transition temperature of a material. Modulus−temperature relationship plays a critical role in determining the heat deflection temperature. HDT occurs at a deformation, which is directly proportional to the load applied and inversely proportional to the modulus.[27] We can also correlate the improvement in the HDT values for the PHBV- and PP-based composites to the higher storage modulus (*E′*) values of these composites at elevated temperature as compared to their neat polymers (Table 3). The PHBV-based composite was found to have an HDT value equivalent to that of the PP-based composite at 40 wt % loading of RCF.

Coefficient of Linear Thermal Expansion. Figure 4 also shows the variation of the coefficient of linear thermal expansion (CLTE) values of the PHBV- and PP-based composites with the incorporation of increasing content of RCF. A low CLTE value is a highly desirable property for a material, when it is used in combination with other material, for example, in electronic packaging. Incorporation of the low-expansion filler in a polymer is an effective way to reduce its thermal expansion. There was a steady decrease in the CLTE values of both PHBV- and PP-based composites with the addition of RCF. The CLTE value of the PHBV-based composites was decreased by ∼70% with the incorporation of 40 wt % RCF. On the other hand, the CLTE value of the PP-based composites was decreased by around ∼43% at similar fiber loading. In a related text on thermal expansion of polymer, van Krevelen[28] suggested that the molar thermal expansivity of a polymer is related to the van der Waals volume of the repeat unit of a polymer. Bondi[29] defined van der Waals volume as volume occupied by a molecule, which is impenetrable by the other molecules having thermal energy at ordinary temperature. So it was impossible for macro-sized fiber to penetrate such a small volume of the polymer and cause the reduction in thermal expansion. Thermal expansion of composites is also affected by the filler/matrix interaction. A strong fiber−matrix interaction restricts the mobility of the polymer chains adhered to the fiber surface, thus helping in reducing the thermal expansion.[30] In the present case, the reduction in coefficient of linear thermal expansion of PHBV- and PP-based composites was primarily because of poor polymer chain mobility of PHBV and PP due to the mechanical constraints developed in the presence of RCF. The larger reduction in the CLTE value of PHBV-based composites as compared to PP-based composites could be due to presence

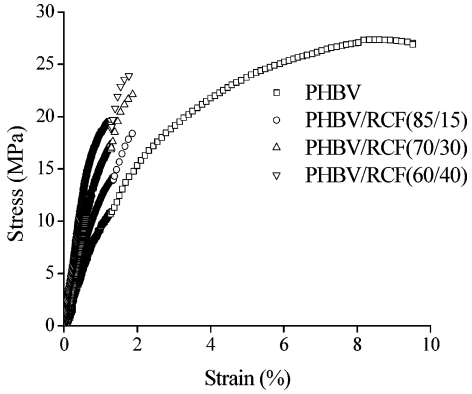

Figure 5. Stress−strain curves of PHBV and its composites obtained from tensile test.

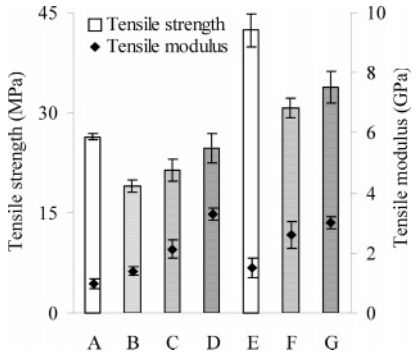

Figure 6. Tensile strength and modulus of PHBV, PP, and their composites: (A) PHBV/RCF (100/0); (B) PHBV/RCF (85/15); (C) PHBV/RCF (70/30); (D) PHBV/RCF (60/40); (E) PP/RCF (100/0); (F) PP/RCF (70/30); (G) PP/RCF (60/40).

of interaction between PHBV and recycled cellulose fibers owing to their relatively polar nature and possible hydrogen-bonding interaction.

Tensile Properties. The tensile properties of the neat PHBV and its composites were evaluated and compared with the RCF-reinforced PP composites. Figure 5 shows the stress−strain curves of PHBV and its composites. The comparative tensile strength and modulus of PHBV, PP, and their composites are shown in Figure 6. Mechanical properties of a short-fiber-reinforced composite depend on the number of factors such as fiber volume, fiber aspect ratio, fiber−matrix adhesion, and fiber orientation.[31] Tensile strength is more dependent on the matrix and the compatibility between fiber and the matrix, while tensile modulus is influenced more by the fiber impregnation and fiber aspect ratio. The stress−strain behavior (Figure 5) of the PHBV-based composite showed that there was a transition from the soft and tough nature of PHBV to the stiff and brittle behavior of PHBV-based composites. The tensile modulus of PHBV-based composite was improved by 220% at 40 wt % fiber content, 3.2 GPa, when compared with neat PHBV, 1.0 GPa. The tensile strength of the PHBV-based composites was first decreased from 26 MPa (neat PHBV) to 19 MPa with addition of 15 wt % RCF. There was an increase in the tensile strength values of PHBV-based composites afterward with the addition of 30 and 40 wt % RCF. This can be explained by the fact that, at low fiber volume, the matrix was not restrained and high strain occurs in the matrix at lower stresses, causing debonding. When fiber volume was above a critical value, the matrix was restrained, resulting in lower strain at comparatively higher stresses.[32] The tensile modulus of PHBV-based composites (3.2 GPa) was found to be higher than that of PP-based composites (3.0 GPa) at 40 wt % RCF. This was a significant result as the tensile modulus of the neat PHBV, 1.0 GPa, was even lower than the tensile modulus of neat PP, 1.5 GPa. This can be explained on the basis of better compatibility and dispersion of RCF in the PHBV matrix as compared to the PP matrix, leading to the superior stress transfer ability in the PHBV-based composite compared with the PP-based composites.

Theoretical Modeling of Tensile Modulus of PHBV-Based Composites. Halpin−Tsai and Tsai−Pagano equations[33−35] were used to determine the theoretical values of the tensile modulus of RCF-reinforced PHBV composites. Cellulose fibers have variable stiffness values due to their origin, constituents, and processing history. Zadorecki et al.[36] determined the elastic moduli of the cellulose fiber using micromechanical relationships for the short-fiber-reinforced composites. This work reported the elastic moduli of cellulose fiber in the range of 18−32 GPa. We selected the elastic modulus value of 18 GPa of cellulose fiber for the theoretical treatment. The reason for this selection was that the recycled cellulose fiber chosen in the present study was expected to have lower stiffness value than the virgin cellulose fiber due to its low cellulose content, variability, mechanical pulping, chemical treatment (bleaching, inking, deinking, etc.) and the multiple processing. The density of PHBV and RCF was 1.25 and 1.20 gm/cm^3, respectively, and the average aspect ratio of RCF was ∼40. Halpin−Tsai equations can predict the theoretical values of longitudinal and transverse moduli of the aligned short fiber composites.

The equations for the longitudinal (E_L) and transverse (E_T) moduli can be written as

$$E_L = E_m \frac{1 + \xi \eta_L V_f}{1 - \eta_L V_f} \quad (1)$$

$$E_T = E_m \frac{1 + 2\eta_T V_f}{1 - \eta_T V_f} \quad (2)$$

where

$$\eta_L = \frac{(E_f/E_m) - 1}{(E_f/E_m) + \xi} \quad (3)$$

$$\eta_T = \frac{(E_f/E_m) - 1}{(E_f/E_m) + 2} \quad (4)$$

Here E_m and E_f are the elastic moduli of the matrix and fiber, respectively, and V_f is the fiber volume fraction. ξ is a measure of the geometry of reinforcement. If the fiber is rectangular in cross-section, then ξ may be calculated as

$$\xi = 2(l/d) \quad (5)$$

Here l/d is the aspect ratio of the reinforcement. The Tsai−Pagano eq 6 can be used to predict the elastic moduli of a composite having randomly oriented fibers:

$$E_{random} = {}^3/_8 E_L + {}^5/_8 E_T \quad (6)$$

Here E_{random} is the elastic modulus of composite having randomly oriented fibers. A comparison between theoretical and experimental tensile modulus of PHBV composites as a function of fiber volume fraction is given in Figure 7. There was considerable deviation in experimental values as compared to theoretical values of tensile modulus for RCF-reinforced PHBV composites. This was an expected result because of the low cellulose content (∼75%) of recycled cellulose fiber used in

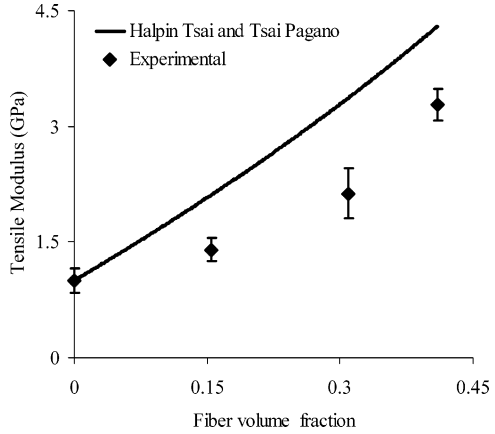

Figure 7. Comparison of experimental and theoretical tensile modulus of PHBV/RCF composites as a function of recycled cellulose fiber volume fraction.

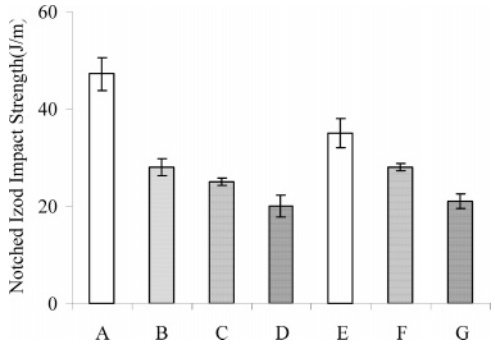

Figure 8. Notched izod impact strength of PHBV, PP, and their composites: (A) PHBV/RCF (100/0); (B) PHBV/RCF (85/15); (C) PHBV/RCF (70/30); (D) PHBV/RCF (60/40); (E) PP/RCF (100/0); (F) PP/RCF (70/30); (G) PP/RCF (60/40).

the study. Recycled cellulose fibers were expected to have large variation in their fibril angle and aspect ratios, which could have reduced their reinforcing ability in PHBV-based composites.

Impact Strength. Figure 8 shows the values of notched izod impact strength of the PHBV- and PP-based composites. The notched izod impact strength of both PHBV- and PP-based composites was found to decrease with increasing amount of recycled cellulose fibers in the composites. The impact strength of neat PHBV was 47 J/m, which was reduced to 20 J/m with incorporation of 40 wt % RCF. The interfacial adhesion, fiber pullout, and mechanism to absorb energy are some of the important parameters in determining the impact strength of short fiber-reinforced composites.[37] The nature of composite, fibers, and type of impact test are the critical factors for the increase or decrease in the apparent impact strength. The possible reason for the decrease in the impact strength could be the reduced plastic deformation of PHBV and PP matrix in the presence of stiff cellulose fibers. The stress−strain curves (Figure 5) of PHBV-based composites depicted a decrease in elongation at break and in the area under the stress−strain curves with increasing amount of RCF in the PHBV matrix. The decrease in the area under stress−strain curves suggested that there was a decrease in the toughness of the PHBV-based composites. Another theory pertaining to the impact strength of the composites suggest that stress concentration caused poor fiber−matrix adhesion around areas of fiber ends, and the region where fiber are in contact with each other provides a low-energy path for crack propagation, thus leading to the decrease in the impact strength of the composites.[38]

Morphology of Composites. The morphology of RCF and

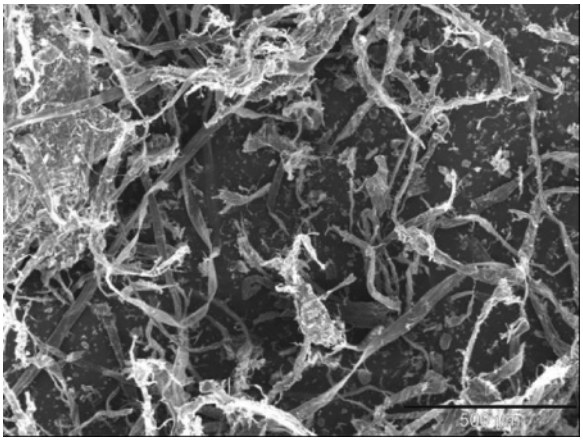

Figure 9. SEM photomicrograph of recycled cellulose fibers (RCF); scale bar = 500 μm.

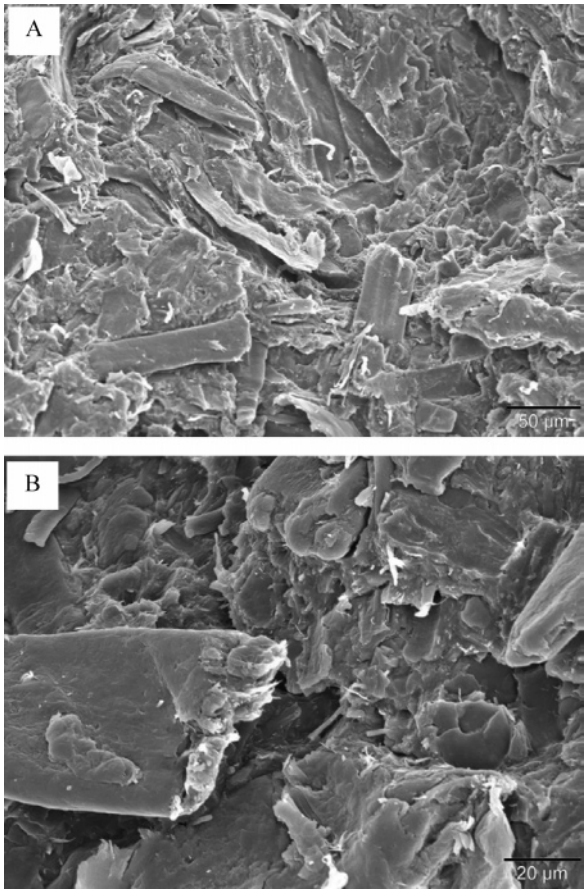

Figure 10. SEM photomicrographs of PHBV/RCF (60 wt %/40 wt %) composite, (A) low magnification (300×, 50 μm) and (B) high magnification (800×, 20 μm).

of PHBV- and PP-based composites were evaluated with the help of scanning electron microscopy (SEM). The SEM photomicrograph of the recycled cellulose fiber is shown in Figure 9. The SEM photomicrograph revealed large-scale variations in the aspect ratio and the morphology of RCF. These variations can be accounted to the different sources and the processing history of the fibers present in the composition of RCF. The impact fractured samples of the PHBV- and PP-based composite having 40 wt % RCF were chosen for analysis of the fiber−matrix adhesion, fiber dispersion, and pullouts in the respective matrices. Figures 10 and 11 present SEM photomicrographs of PHBV- and PP-based composites. The SEM photomicrographs of PHBV- and PP-based composites also indicated variation in

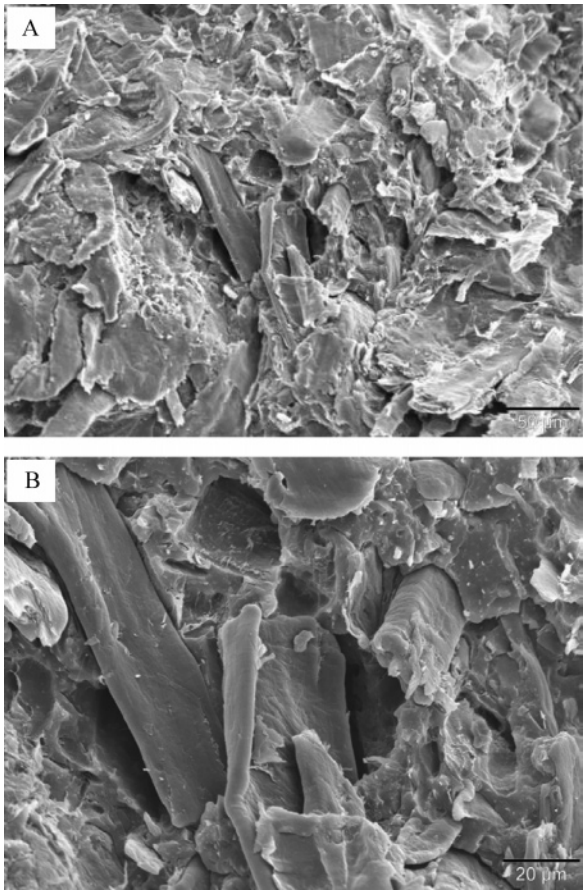

Figure 11. SEM photomicrographs of PP/RCF (60 wt %/40 wt %) composite, (A) low magnification (300×, 50 μm) and (B) high magnification (800×, 20 μm).

the morphology of recycled cellulose fibers. The SEM photomicrographs were not able provide information regarding fiber dispersion due to the variability in the morphology of the RCF. The low-magnification images of the PHBV- and PP-based composites did not provide much information regarding the interfacial adhesion, probably due to small fiber size. The high-magnification SEM photomicrographs of the PHBV- and PP-based composites revealed fiber pullouts in both composites. The presence of bare fibers was relatively more in the PP-based composites as compared to the PHBV-based composites. The high-magnification SEM photomicrographs of the PP-based composite also revealed debonding at the areas of contact between fiber and matrix. The relatively polar nature of the PHBV as compared to the PP could have provided relatively better compatibility for the polar RCF. A strong interfacial adhesion is required between fiber and matrix for the effective transfer of stress from the matrix to fibers.[39] The relatively better compatibility of the recycled cellulose fiber with the PHBV matrix can be correlated with the superior enhancement in properties such as tensile modulus and storage modulus (E') and the large reduction in coefficient of linear thermal expansion (CLTE) values for the PHBV-based composites as compared to the PP-based composites.

Conclusion

This study was focused on the fabrication of low-cost value-added biodegradable composite materials from a recycled biobased product such as recycled cellulose fibers (RCF) and a bacterial polyester, poly(3-hydroxybutyrate-*co*-3-hydroxyvalerate) (PHBV). The incorporation of RCF had brought considerable improvement in the properties of PHBV such as tensile and storage moduli and heat deflection temperature (HDT). The coefficient of linear thermal expansion (CLTE) value of PHBV was reduced significantly upon reinforcement with RCF. The thermomechanical properties of PHBV-based composite had competed favorably with PP-based composite at similar fiber loadings. Scanning electron microscopy (SEM) revealed better compatibility of the RCF in the PHBV matrix as compared to the PP matrix. The lower processing temperature and the shorter cycle time in processing of PHBV-based composite were beneficial in avoiding the attrition and degradation of the cellulosic fibers. The possibilities of high fiber loading in the PHBV-based composites can reduce the amount of expansive PHBV resin in the composite formulations. The biodegradable nature and competent properties of RCF-reinforced PHBV composites can provide a sustainable alternative to conventional thermoplastic-based materials.

Acknowledgment. Financial support from NSF Award DMI-0400296, PREMISE-II: Design and engineering of green composites from biofibers and bioplastics, and NSF 2002 Award DMR-0216865, under the Instrumentation for Materials Research (IMR) Program, is gratefully acknowledged. We also express our appreciation to CreaFill Fibers Corp. (Chestertown, MD), Biomer (Germany), and Basell Polyolefins (Elkton, MD) for supplying recycled cellulose fibers, PHBV, and PP, respectively. We thank the Composite Material and Structures Center, Michigan State University, for allowing us to use its facilities and instruments. We are also thankful to Carol Flegler, Center for Advanced Microscopy, Michigan State University, for helping in scanning electron microscopy (SEM).

References and Notes

(1) Mohanty, A. K.; Misra, M.; Drzal, L. T. Sustainable Biocomposites from Renewable Resources: Opportunities and Challenges in Green Materials World. *J. Polym. Environ.* **2002**, *10*.
(2) Sanadi, A. R.; Caufield, D. F.; Jacobson, R. E.; Rowell, R. M. Renewable Agriculture Fibers as Reinforcing Fillers in Plastics: Mechanical Properties of Kenaf Fiber−Polypropylene Composites. *Ind. Eng. Chem. Res.* **1995**, *34* (5).
(3) Mohanty, A. K.; Drzal, L. T.; Misra, M. Novel Hybrid Coupling Agent As Adhesion Promoter in Natural Fiber Reinforced Powder Polypropylene Composites. *J. Mater. Sci. Lett.* **2002**, *21*, 1885−1888.
(4) Lu, J. Z.; Wu, Q.; Negulescu, I. I. Wood Fiber/ High-Density-Polyethylene Composites: Coupling Agent Performance. *J. Appl. Polym. Sci.* **2005**, *96*, 93−102.
(5) Mohanty, A. K.; Misra, M.; Hinrichsen, G. Biofibres, biodegradable polymers and biocomposites: An overview. *Macromol. Mater. Sci. Eng.* **2000**, *276/277*, 1−24.
(6) Mohanty, A. K.; Misra, M.; Drzal, L. T. *Compos. Interface* **2001**, *8*, 313−343.
(7) Lenz, R. W.; Marchessault, R. H. Bacterial Polyester: Biosynthesis, Biodegradable Plastics and Biotechnology. *Biomacromolecules* **2005**, *6* (1).
(8) Marchessault, R. H.; Coulombe, S.; Morikawa, H.; Okamura, K.; Revol, J. F. Solid-state properties of poly-beta-hydroxybutyrate and its oligomers. *Can. J. Chem.* **1981**, *59*, 38−44.
(9) Barham, P. J.; Keller, A.; Otum, E. I.; Holmes, P. A. Crystallization and morphology of a bacterial thermoplastic−Poly-3-Hydroxybutyrate. *J. Mater. Sci.* **1984**, *19*, 2781−2794.
(10) Holmes, P. A. In *Developments in Crystalline Polymers*; Basset, D. C., Ed.; Elsevier Applied Science: London, 1988; Vol. 2, pp 1−65.
(11) Billingham, N. C.; Henman, T. J.; Holmes, P. A. In *Developments in Polymer Degradation 7*; Grassie, N., Ed.; Applied Science Publishers: London, Chapter 3.
(12) Kunioka, M.; Tamaki, A.; Doi, Y. Crystalline and Thermal Properties of Bacterial Copolyesters: Poly(3-hydroxybutyrate-*co*-3-hydroxyvalerate) and Poly(3-hydroxybutyrate-*co*-4-hydroxybutyrate). *Macromolecules* **1989**, *22*, 694−697.

(13) Biddlestone, F.; Harris, A.; Hay, J. N.; Hammond, T. Physical Aging of Amorphous Poly(hydroxybutyrate). *Polym. Int.* **1996**, *39*, 221−229.
(14) Bauer, H.; Barham, P. J. *J. Mater. Sci.* **1988**, *26*, 241.
(15) Reinsch, V. E.; Kelley, S. S. Crystallization of Poly (hydroxybutyrate-*co*- hydroxyvalerate) in wood fiber reinforced composites. *J. Appl. Polym. Sci.* **1997**, *64* (9), 1785−1796.
(16) Luo, S.; Netravalli, A. N. Interfacial and Mechanical Properties of Environment-friendly "Green" Composites made from pineapple fibers and poly(hydroxybutyrate-*co*-valerate) Resin. *J. Mater. Sci.* **1999**, *34*, 3709−3719.
(17) Mohanty, A. K.; Khan, M. A.; Hinrichsen, G. Surface Modification of Jute and Its Influence on Performance of Biodegradable Jute fabric-Biopol Composite. *Compos. Sci. Technol.* **2000**, *60*, 1115−1124.
(18) Espert, A.; Camacho, W.; Karlson, S. Thermal and Thermo-mecanical Properties of Biocomposites made from Modified Recycled Cellulose and Recycled Polypropylene. *J. Appl. Polym. Sci.* **2003**, *89*, 2353−2360.
(19) English, B. Meeting Society Challenge: Value Added Products From Recycled Materials. Pacific Rim Bio-Based Composites Symposium, Rotorua, New Zealand, November 9−13, 1992.
(20) Huda, M. S.; Drzal, L. T.; Misra, M.; Mohanty, A. K.; Williams, K.; Mielewiski, D. F. A Study on Biocomposite from Recycled Newspaper Fiber and Poly (lactic acid). *Ind. Eng. Chem. Res.* **2005**, *44* (15), 5593−5601.
(21) Huda, M. S.; Mohanty, A. K.; Drzal, L. T.; Misra, M.; Schut, E. "Green" composite from recycled cellulose and Poly(lactic acid): Physicomechanical and morphological evaluation. *J. Mater. Sci.* **2005**, *40* (16), 4221−4229.
(22) http://www.creafill.com/creamix.htm.
(23) Zhang, J.; McCarthy, S.; Whitehouse, R. Reverse Temperature Injection Molding of Biopol and Effect on Its Properties. *J. Appl. Polym. Sci.* **2004**, *94*, 483−491.
(24) Shanks, R. A.; Hodzic, A.; Wong, S. Thermoplastic Biopolyester Natural Fiber Composites. *J. Appl. Polym. Sci.* **2004**, *91*, 2114−2121.
(25) Gatenholm P.; Mathiasson, A. Biodegradable Natural Composites, II. Synergistic Effects of Processing Cellulose with PHB. *J. Appl. Polym. Sci.* **1994**, *51*, 1231−1237.
(26) Turi, E. A. *Thermal characterization of polymeric materials*, 2nd ed.; Elsevier Science & Technology Books; New York, 1997.
(27) Nielsen, E. L. In Mechanical properties of Polymers and Composites; Marcel Dekker: New York, 1976; Vol. 2, p 344.
(28) van Krevelen, D. W. Volumetric Properties. In *Properties of Polymers: Their Estimation and Correlation with chemical structure*; Elsevier: Amsterdam, Oxford, New York, 1976; Chapt. 4, pp 67−74.
(29) Bondi, A. van der Waals volume and radii. *J. Phys. Chem.* **1964**, *68*, 441−451.
(30) Yang, H. S.; Wolcott, M. P.; Kim, H. S.; Kim, H. J. Thermal Properties of Lignocellulosic Filler-Thermoplastic Polymer Bio-Composites. *J. Therm. Anal. Calorim.* **2005**, *82*, 157−160.
(31) Saheb, D. N.; Jog, J. P. Natural Fiber Polymer Composites: A Review. *Adv. Polym. Technol.* **1999**, *18* (4), 351−363.
(32) Joseph, S.; Jacob, M.; Thomas, S. Natural Fiber-Rubber Composites and Their Applications. In *Natural Fibers, Biopolymers and Biocomposites*; Mohanty, A. K., Misra, M., Drzal, L. T., Eds.; CRC Press: Boca Raton, FL, 2005.
(33) Halpin, J. C.; Tsai, S. W. Effects of Environmental Factors on Composite Materials. AFML-TR 67-423, 1969.
(34) Halpin, J. C.; Kardos, J. C. *Polym. Eng. Sci.* **1976**, *16* (5), 344.
(35) Tsai, S. W.; Pagano, N. J. *Composite Material Workshop*; Technomic Publishing Co.: New York, 1968; pp 233−253.
(36) Zadorecki, P.; Karnerfors, H. Cellulose Fibers as Reinforcement in Composites: Determination of the stiffness of Cellulose Fibers. *Compos. Sci. Technol.* **1986**, *27*, 291−303.
(37) Tobias, B. C. *Proceedings of the International Conference on Advanced Composite Materials*; Minerals, Metals & Materials Society (TMS): Warrendale, PA, 1993; p 623.
(38) Nielsen, E. L. In *Mechanical Properties of Polymer and Composites*; Marcel Dekker: New York, 1976; Vol. 2, pp 483−484.
(39) Herrera Franco, P. J.; Gonzalez, A. V. Fiber−Matrix Adhesion in Natural Fiber Composites. In *Natural Fibers, Biopolymers and Biocomposites*; Mohanty, A. K., Misra, M., Drzal, L. T., Eds.; CRC Press: Boca Raton, 2005.

BM050897Y